

# Three-dimensional optical metrology with color-coded extended depth of focus

E. Hasman

*Faculty of Mechanical Engineering, Technion—Israel Institute of Technology, Haifa 32000, Israel*

S. Keren, N. Davidson, and A. A. Friesem

*Department of Physics of Complex Systems, Weizmann Institute of Science, Rehovot 76100, Israel*

Received December 21, 1998

A novel method of rapid three-dimensional optical metrology that is based on triangulation of a configuration of color-coded light stripes is presented. The method exploits polychromatic illumination and a combined diffractive–refractive element, so the incident light is focused upon a stripe that is axially dispersed, greatly increasing the depth-measuring range without any decrease in the axial or the lateral resolution. The discrimination of each color stripe is further improved by spectral coding and decoding techniques. An 18-fold increase in the depth of focus was experimentally obtained while diffraction-limited light stripes were completely maintained. © 1999 Optical Society of America

*OCIS codes:* 100.6890, 120.3940, 050.1940.

The increasing need for noncontact three-dimensional (3-D) profile measurements has already led to the development of several electro-optic measuring systems<sup>1</sup> based on structured light triangulation. The simplest of these systems projects a single point of light from the source onto the surface of a 3-D object. The single-point triangulation approach is relatively inexpensive and capable of high resolution. However, the measurement of 3-D surfaces involves lengthy time-consuming axial and lateral scanning, which is often impractical. A more-complicated system involves the projection of a light stripe onto the surface of the object and a two-dimensional detector array. In this system, only one lateral scan in the direction perpendicular to the stripe is needed, thereby reducing the overall measurement time.<sup>2</sup>

A further decrease in measurement time is possible if one resorts to lenses of relatively low numerical aperture, which have a longer depth of focus, so that there is no need for axial scanning. Here, the lateral resolution decreases because of the inherent increase of the size of the light spot on the surface. It is possible to determine the center of the spot with much higher accuracy than the spot size by use of complicated numerical techniques.<sup>3</sup> Such techniques can reasonably overcome errors that are due to statistical noises, such as shot noise, CCD amplifier noise, and errors owing to CCD pixel response nonuniformity and quantization. However, these techniques are very sensitive to systematic noises such as local changes in the reflectivity or the shape of the object (e.g., a short radius of curvature cannot be adequately dealt with).

For a single-point triangulation approach it is possible to use aspherical optical elements, such as axicon<sup>4,5</sup> or axilens,<sup>6</sup> that have both high resolution and long focal depth. Such aspherical elements have two main problems. First, the peak-to-background ratio (PBR) is relatively low compared with those of conventional diffraction-limited lenses. Second, the principle of operation of aspherical elements relies greatly on the singularity of the optical axis in a circular symmetry

and thus cannot be generalized to a light stripe with a long depth of focus. In particular, with light-stripe geometry, unacceptable high sidelobes would result.

In this Letter we present a novel approach to light-stripe triangulation configuration that allows parallel, fast, real-time 3-D surface metrology with a large depth-measuring range and high axial and lateral resolution. The method is based on a color-coded arrangement that exploits polychromatic illumination and a cylindrical element that disperses the incident light along the axis, which increases the depth-measuring range without any decrease in the axial or the lateral resolution. For the cylindrical element we investigated a combined diffractive–refractive optical element in which many light stripes, each of a different wavelength, are simultaneously focused at different focal lengths, forming a rainbow light sheet. We also investigated a color-decoding technique in which a spectral filter matched in parallel with the entire wavelength distribution of the light sheet is incorporated into the detection part of the system. This technique allowed us to increase significantly the depth of focus while maintaining a diffraction-limited stripe width with extremely small sidelobes, comparable with those of conventional refractive lenses.

The principle of our color-coded approach is shown in Fig. 1. The polychromatic light source can be either a white-light source or an ultrashort pulsed laser that produces relatively a large spectral bandwidth. A collimating lens forms plane waves that are then focused by axially dispersing optics (ADO), such as a cylindrical diffractive optical element or a combined diffractive–refractive optical element. The ADO forms a rainbow light sheet that consists of light stripes of different wavelengths at different distances from the lens. An object whose depth is smaller than the rainbow focal depth,  $\Delta F$ , intersects the rainbow light sheet, and the intersection profile of the object is then imaged with an off-axis configuration (at an angle  $\theta$  from the illumination optical axis) to a two-dimensional array CCD detector. We process the detected data by computer to

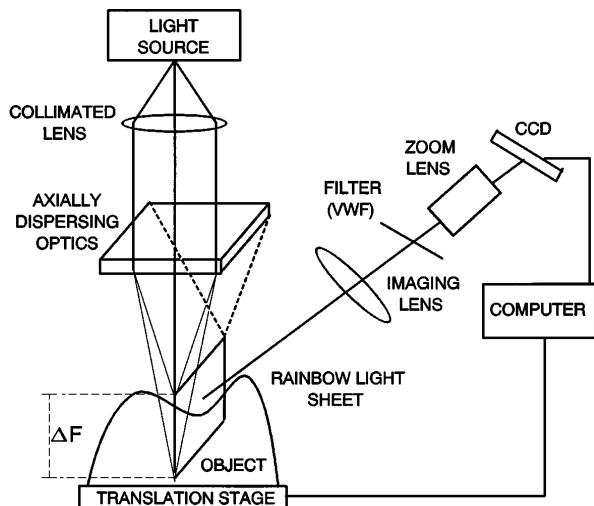


Fig. 1. Color-coded light-stripe triangulation system.

obtain the profile in virtually real time. After a line is detected, a computer-controlled stepper motor shifts the object to obtain another line, and so on, until a complete 3-D profile of the object is obtained. Although the rainbow light sheet is composed of thin stripes (limited by the diffraction) of the individually focused wavelengths, each stripe is surrounded by background light of other wavelengths. Thus, the detected profile is relatively broad. We can significantly narrow this profile by suppressing the background light and allowing only light of the proper (focused) wavelength to be detected at each object depth. This light selection is achieved by insertion of an interference filter whose transmitted wavelength is spatially nonuniform into the detection path. With such a variable-wavelength filter (VWF) optimal performance is obtained when the spread and the specific wavelength location match those of the light from the ADO. When the match is exact, it is possible to obtain diffraction-limited resolution over the entire depth of focus without any scanning.

To test our approach we designed and built a color-coded triangulation arrangement. For the illumination source we used a 75-W xenon-arc lamp with a continuous spectrum ranging from 400 to 700 nm and used heat-absorbing glass to reduce the IR radiation. The light emerging from the lamp was focused by a parabolic mirror onto a slit whose aperture was  $40\ \mu\text{m}$ , from which it was collected and formed into a rainbow light sheet with a  $2-f$  configuration of lenses. The first lens in the  $2-f$  configuration was an achromatic lens with a 500-mm focal length, and the second lens was the ADO. The ADO was combination of a cylindrical refractive lens with focal length  $f_r = 496\ \text{mm}$  and an adjacent quadratic-phase diffractive cylindrical lens with focal length  $f_d = 1040\ \text{mm}$ , both at  $\lambda_0 = 529\ \text{nm}$ . The diffractive lens was recorded by use of a computer-generated mask, photolithographic techniques, and reactive-ion etching to form a 16-binary-level element on a fused-silica substrate.<sup>7</sup> The combined ADO lens configuration had an aperture of diameter  $D = 9\ \text{mm}$  and was designed to have an approximately linear dispersion so that it would match

exactly the linear dispersion of the commercially available VWF (Schott VERIL S 60) that was used. The measured and the calculated dispersion results for the ADO are shown in Fig. 2. As is evident, there is good agreement between the measured and the predicted results. The measured combined focal length of the ADO at  $\lambda_0 = 529\ \text{nm}$  was  $F_0 = 326\ \text{mm}$ , and the rainbow focal depth was  $\Delta F = 48\ \text{mm}$ . In comparison, the focal depth of a conventional refractive lens is  $\delta F \approx 4\lambda_0 F_{\#}^2 \approx 2.7\ \text{mm}$  (80% of the maximal axial intensity) at a similar  $f$ -number,  $F_{\#} = 36$ . Therefore, the enlarging factor of the focal depth,  $M_0$ , which is defined as the ratio of the rainbow focal depth of the ADO,  $\Delta F$ , to that of a conventional lens focal depth,  $\delta F$ , is  $M_0 = \Delta F / \delta F \approx 18$ . Figure 2 also shows the measured wavelength transmittance band and the dispersion of the linear VWF. The horizontal distance between the two solid lines represents the spectral width of the filter,  $\delta\lambda$ , at each focal-length position. The VWF discrimination,  $M_f$ , is defined by the number of wavelengths that can be discriminated. Specifically, it is the total spectral range,  $\Delta\lambda \approx 300\ \text{nm}$ , divided by the spectral width of the filter,  $\delta\lambda \approx 15\ \text{nm}$ , which yields  $M_f = \Delta\lambda / \delta\lambda \approx 20$ . The measured dispersion of the ADO matches the transmittance band of the linear VWF. The optimal filter parameter  $M_f^{\text{opt}}$  can be obtained from the axial resolving power of the ADO as  $M_f^{\text{opt}} \approx M_0$ . Such a value of  $M_f^{\text{opt}}$  yields a sharp image of the object profile, with a near-diffraction-limited focused linewidth.

To test the experimental arrangement we performed a series of measurements of a flat object placed at an angle so that the entire focal range was included in the measurements. First, we measured the intensity cross-section distributions of the reflected light at the start, middle, and end of the ADO focal range ( $z = 299\ \text{mm}$ ,  $z = 323\ \text{mm}$ , and  $z = 347\ \text{mm}$ , respectively). Figures 3(a) and 3(b) show the measured and the calculated intensity cross sections, respectively.<sup>8</sup> These results show that a diffraction-limited linewidth of

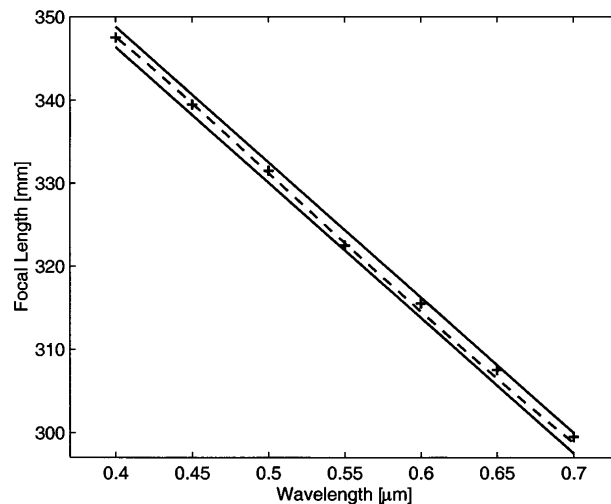


Fig. 2. Measured (+) and calculated (dashed line) dispersion of the ADO, combined diffractive-refractive lens, and the wavelength transmittance band and the dispersion of the linear variable wavelength filter (solid lines).

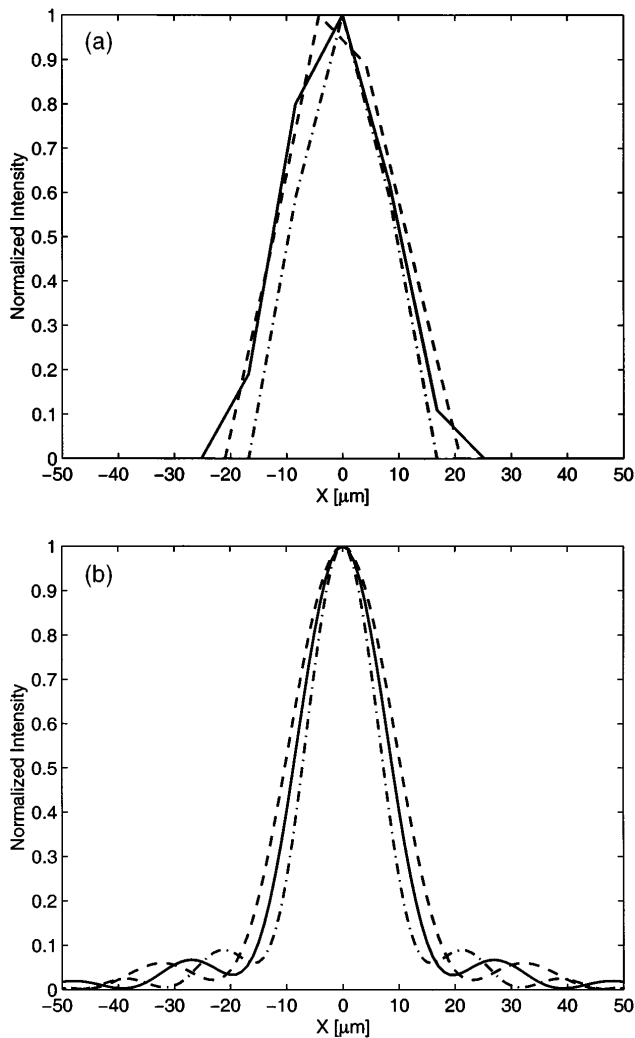


Fig. 3. Measured (a) and calculated (b) intensity cross sections at three positions along the focal range: dashed curve,  $z = 299$  mm; solid curve,  $z = 323$  mm; dashed-dotted curve,  $z = 347$  mm.

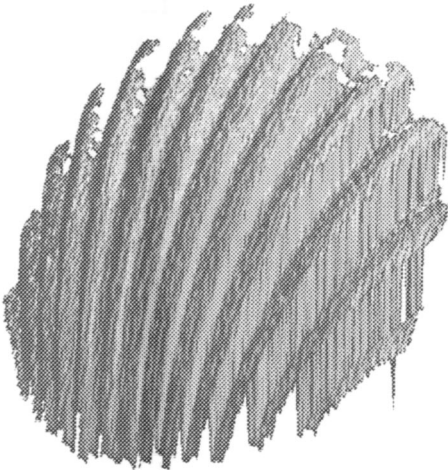


Fig. 4. Measured profile of a seashell.

$\sim \Delta x \cong 20 \mu\text{m}$  at FWHM is maintained throughout the focal range, with good agreement between experiment and theory. These results thus indicate that near-perfect matching between the ADO and the filter

dispersions was indeed obtained. We also measured the intensity cross sections of the light stripe along the focal range without the VWF. The results revealed that a narrow peak with near-diffraction-limited size is still obtained throughout the focal region  $\Delta F$  but with a PBR of only 1.5, also in agreement with our calculation. This PBR sets a limit for the allowed noise level that can exist in the system without significantly degrading its accuracy to 50% of the maximal background value. With a VWF, however, the PBR improves significantly to  $\sim 15$ .

For a complete measured profile of the flat object, we used an analog CCD with 500 by 700 pixels; each pixel acquired  $\sim 68 \mu\text{m}$  of the focal range. We also exploited a centroid (center-of-gravity) algorithm to detect the center of the output light stripe and corrected optical distortions of the imaging configuration by appropriate calibration. We found that the deviation of the measured result from the expected linear line is  $\pm 0.2$  pixel error for most of the focal range. This deviation corresponds to a lateral and depth resolution of  $\delta x \cong \delta z \cong 13 \mu\text{m}$  with focal range  $\Delta F \cong 48$  mm. Thus, the number of resolving-depth steps is  $\Delta F / \delta z = M_0 \delta F / \delta z \cong 3700$ . We can further improve these results by resorting to a digital CCD camera with more pixels and low noise to permit submicrometer resolution over the extended focal range. Note that with a conventional triangulation approach (without color coding and decoding), and a noise level comparable with that used here, the resolving-depth steps would be only  $\delta F / \delta z \cong 200$ .

Finally, in our experiments we used real-time software to process the data from the CCD camera and calculate the center of the detected stripes. An entire line cross section of the object's profile could be obtained at a video rate, permitting fully automatic and fast 3-D measurement of the overall surface of a 3-D object. Figure 4 is an example of 3-D surface mapping of a seashell, which was obtained by our color-coded profilometer, with the VWF, in only  $\sim 0.5$  s.

E. Hasman's e-mail address is mehasman@tx.technion.ac.il.

## References

1. R. G. Dorsch, G. Häusler, and J. M. Herrmann, *Appl. Opt.* **33**, 1306 (1994).
2. D. W. Manthey, K. N. Knapp II, and D. Lee, *Opt. Eng.* **33**, 3372 (1994).
3. P. Seitz, *Opt. Eng.* **27**, 535 (1988).
4. B. Z. Dong, G. Z. Yang, and B. Y. Gu, *J. Opt. Soc. Am. A* **13**, 97 (1996).
5. G. Bickel, G. Häusler, and M. Maul, *Opt. Eng.* **24**, 975 (1985).
6. N. Davidson, A. A. Friesem, and E. Hasman, *Opt. Lett.* **16**, 523 (1991).
7. E. Hasman, N. Davidson, and A. A. Friesem, *Opt. Lett.* **16**, 423 (1991).
8. We calculated the intensity of each wavelength by multiplying a Fresnel diffraction integral by the VWF response and taking into account the dispersion relation of the ADO. The total intensity was obtained by integration of those intensities over the entire spectrum of the source.